Environ. Res. Lett. **6** (2011) 034036 (8pp) doi:10.1088/1748-9326/6/3/034036

Risk of severe climate change impact on the terrestrial biosphere

Ursula Heyder[1,2], **Sibyll Schaphoff**[1], **Dieter Gerten**[1] **and Wolfgang Lucht**[1,3]

[1] Potsdam Institute for Climate Impact Research, Telegraphenberg A62, 14473 Potsdam, Germany
[2] International Max Planck Research School on Earth System Modelling, Hamburg, Germany
[3] Department of Geography, Humboldt University, Berlin, Germany

E-mail: Ursula.Heyder@pik-potsdam.de and Sibyll.Schaphoff@pik-potsdam.de

Received 27 June 2011
Accepted for publication 6 September 2011
Published 26 September 2011
Online at stacks.iop.org/ERL/6/034036

Abstract
The functioning of many ecosystems and their associated resilience could become severely compromised by climate change over the 21st century. We present a global risk analysis of terrestrial ecosystem changes based on an aggregate metric of joint changes in macroscopic ecosystem features including vegetation structure as well as carbon and water fluxes and stores. We apply this metric to global ecosystem simulations with a dynamic global vegetation model (LPJmL) under 58 WCRP CMIP3 climate change projections. Given the current knowledge of ecosystem processes and projected climate change patterns, we find that severe ecosystem changes cannot be excluded on any continent. They are likely to occur (in >90% of the climate projections) in the boreal–temperate ecotone where heat and drought stress might lead to large-scale forest die-back, along boreal and mountainous tree lines where the temperature limitation will be alleviated, and in water-limited ecosystems where elevated atmospheric CO_2 concentration will lead to increased water use efficiency of photosynthesis. Considerable ecosystem changes can be expected above 3 K local temperature change in cold and tropical climates and above 4 K in the temperate zone. Sensitivity to temperature change increases with decreasing precipitation in tropical and temperate ecosystems. In summary, there is a risk of substantial restructuring of the global land biosphere on current trajectories of climate change.

Keywords: ecosystem change, DGVM, climate change, impact metric

S Online supplementary data available from stacks.iop.org/ERL/6/034036/mmedia

1. Introduction

Climate change will have strong impacts on the global terrestrial biosphere, but these have not been well quantified. This is mainly due to large gaps in ecophysiological process understanding, lack of insight into the principles of generalization from case studies (Parmesan 2006), lack of sufficient past precedence or analogues for future climate states (Williams *et al* 2007), and a rather large uncertainty regarding the magnitude and spatial pattern of potential future climate change in climate model projections, particularly with respect to precipitation (Randall *et al* 2007). Ecosystems have a substantial ability to buffer and adapt to changes in external parameters on a number of levels from biogeochemical adaptations to community responses. However, significant ecosystem restructuring, state change or even collapse occur when the limits of system adaptation are approached or passed (Scheffer *et al* 2001, Lenton *et al* 2008). The risk of a potential collapse of parts of the Amazonian rainforest due to decreased precipitation (Betts *et al* 2004), die-back of boreal forests in continental interiors and ingression of woody vegetation into the tundra (Chapin *et al* 2005) are just the most prominent cases being discussed.

Most studies on biospheric climate change impacts focus on one or a few isolated ecosystem processes only (Cramer *et al* 2001, Friedlingstein 2006, Gerten *et al* 2007). However, given the many potential responses of an ecosystem to external pressure and the possibility of homoeostasis in key ecosystem functions through compensatory mechanisms (Ernest and Brown 2011), a comprehensive risk assessment of ecosystem changes should comprise several aspects of ecosystem functioning e.g. Scholze *et al* (2006). We propose to estimate the distance of a potential future ecosystem state under climate change from current conditions by using a new generic metric (Γ) of biogeochemical shifts and vegetation structural changes. We interpret a large value of Γ as an increased risk of ecosystem disruption, arguing that substantial changes in either basic biogeochemical properties or vegetation composition are likely to imply far-reaching, potentially self-amplifying transformations in the underlying system characteristics, food chains and species composition. We base our metric on (a) changes in two major biogeochemical exchange fluxes, those of carbon and water, (b) changes in the material stocks of carbon (biomass) in the system, (c) changes in the proportional relation of carbon and water fluxes to each other, and (d) changes in vegetation composition (functional strategies).

Using this metric Γ, we assess the risk of severe ecosystem changes by the end of the 21st century, addressing the following uncertainties: (i) human induced emission pathways by using three SRES emission scenarios and (ii) climate sensitivity and climate change patterns by using climate projections from 22 General Circulation Models (GCMs) from the World Climate Research Programme's Coupled Model Intercomparison Project (WCRP CMIP3). Ecosystem responses to projected climate changes are quantified with a dynamic global vegetation model (DGVM), LPJmL (Sitch *et al* 2003, Gerten *et al* 2004). DGVMs integrate current knowledge on physiological and ecological ecosystem processes (Woodward *et al* 1995, Foley *et al* 1996, Krinner *et al* 2005) and are the most advanced tools available to simulate ecosystem responses to changes in climate and atmospheric CO_2 on a broad spatial scale. We additionally derive climate response functions for ecosystems in temperate, tropical, cold and dry climate zones, which give an indication of ecosystem vulnerability to climate change that is independent of climate change patterns.

2. Methods

2.1. Ecosystem change indicator

Our proposed metric for ecosystem change, the 'generic ecosystem stability index' Γ, is based on macroscopic variables DGVMs are able to simulate with some confidence as shown in (McGuire *et al* 2001, Thonicke *et al* 2001, Sitch *et al* 2003, Gerten *et al* 2004), assuming that the simulated variables provide sufficient indications of an ecosystem's state, either characterizing the complete ecosystem state or a specific subset of variables (table 1). The distance between the current and a potential future ecosystem state characterizes the change that an ecosystem has to adapt to. The larger this distance, the higher the risk that adaptation fails on short time scales and the system restructures or collapses. Γ captures five dimensions of ecosystem change.

Table 1. Variable subsets used for analysis.

Subset	Variables
Carbon fluxes	Net primary production (NPP), heterotrophic respiration (Rh), fire carbon
Stored carbon	Carbon contained in vegetation and soils
Water fluxes	Transpiration, evaporation, runoff
All	Carbon fluxes, stored carbon, water fluxes, fire frequency, soil water content
Vegetation structure	Composition (plant functional types)

(i) Change in vegetation structure ΔV expressed in terms of ecological strategies, i.e. plant functional types (PFT), as shifts in functional composition have strong impacts on underlying plant and consumer communities and thus on biodiversity, irrespective of biogeochemical performance.
(ii) Relative change of ecosystem state c, expressed as relative change in biogeochemical stocks and fluxes, to quantify the magnitude of local alterations.
(iii) Absolute change of ecosystem state g (compared to the global mean value), as particularly strong changes are more likely to feed back to larger scales (e.g. carbon cycle feedbacks, changes of atmospheric circulation patterns) and imply severe impacts in any ecosystem.
(iv) Shifts in the relative magnitude of key categories of biogeochemical exchange fluxes (e.g. carbon and water) b with respect to each other as an indicator for the risk of qualitative changes in dynamic processes. If there is a severe shift in the simulated balance of functions, there is an increased probability that the existing communities break down and are replaced by new communities.
(v) Change in ecosystem state in relation to natural state variability S, as a system is adapted to the interannual variability it is regularly exposed to and may be vulnerable if it is exceeded.

We calculate and analyse c, g and b (each scaled with a function of their respective change-to-variability ratio $S(x, \sigma_x)$) and ΔV, and a combined metric Γ as the mean of the four components, following the idea that simultaneous changes in several of those dimensions indicate a higher risk of ecosystem destabilization than changes in just one of them:

$$\Gamma = (\Delta V + cS(c, \sigma_c) + gS(g, \sigma_g) + bS(b, \sigma_b))/4. \quad (1)$$

Components S, c, g, b and ΔV are each scaled between 0 (no change) and 1 (very severe change). We define the latter by the following criteria: a magnitude of change exceeding the magnitude of the mean ecosystem state (c and g) or exceeding three standard deviations of natural variability (S), a change in ecosystem composition to a completely different dominating

ecological strategy (e.g. grass versus tree) (ΔV) or an angle between present and future state vectors larger than 60° (b). We consider a value of $\Gamma > 0.3$ a severe impact on an ecosystem (i.e. very severe changes in at least one of the change dimensions or moderate to severe changes in all of them), and a value of $\Gamma < 0.1$ a small impact. For illustrative purposes, we calculated Γ between present-day ecosystems along a latitudinal transect at 20°E (table S1 available at stacks.iop.org/ERL/6/034036/mmedia): Γ is 0.2 between a dry, soil carbon rich boreal mixed forest and a temperate mixed forest, $\Gamma = 0.98$ between a tropical rainforest and a semi-desert and $\Gamma = 0.55$ between a productive, fire dominated, moist savannah and a tropical rainforest. Note that differences in original state and state variability lead to an asymmetric table, the 'direction' of calculation is important.

2.1.1. Change in vegetation structure ΔV. ΔV is calculated using a metric developed by Sykes *et al* (1999), which measures structural dissimilarity of two ecosystems i, j based on their composition in terms of plant life forms k (either trees, grass, or bare ground) and their assigned attributes a_l taking a value of zero or one depending on type (either needleleaved or broadleaved) and phenology (either evergreen or deciduous) of leaves:

$$\Delta V(i,j) = 1 - \sum_k \left\{ \min(V_{ik}, V_{jk})[1 - \sum_l w_{kl}|a_{ikl} - a_{jkl}|] \right\} \tag{2}$$

V_{ik} and V_{jk} are the area fractions covered by life form k in ecosystems i and j. The term $\sum_k \min(V_{ik}, V_{jk})$ adopts a value of 0 if the two systems have no life form in common and a value of 1 if the life form composition is identical. This value is modified for each life form by a term describing attribute similarity, where attributes are weighted equally by $w_{kl} = 0.5$ in our analysis. ΔV takes a value of 0 for ecosystems with identical composition and 1 for completely different systems. Vegetation composition is simulated with the LPJmL model (Sitch *et al* 2003) based on nine PFTs.

2.1.2. Change in ecosystem state. Components c, g, b and S (equation (1)) are calculated in the multi-dimensional phase-space spanned by simulated ecosystem variables v_i consisting of (i) state variables (vegetation carbon stock, soil carbon stock, soil water status), (ii) variables describing fluxes into and out of the system (net primary productivity, soil heterotrophic respiration, transpiration, evaporation, fire carbon emissions) and (iii) variables describing system internal processes (fire frequency). Although Γ is designed to cover the most relevant macroscopic ecosystem features, the choice of variables determines the shape of the phase-space and could be adjusted for specific questions (for details on our model setup and time frame see section 2.4). Every location at any point in time has a corresponding position in this phase-space and can be described by a vector from the origin. For two points in time t_1 and t_2, the corresponding state vectors $\vec{s_1}$ and $\vec{s_2}$ for variables $v_i, i = [1, \ldots, n]$ are:

$$\vec{s_1} = \begin{pmatrix} v_{1,1} \\ v_{2,1} \\ \vdots \\ v_{n,1} \end{pmatrix}, \qquad \vec{s_2} = \begin{pmatrix} v_{1,2} \\ v_{2,2} \\ \vdots \\ v_{n,2} \end{pmatrix}. \tag{3}$$

The distance between points is a measure of similarity between ecosystems, calculated as magnitude of the difference vector $\vec{d}$:

$$d = |\vec{d}| = |\vec{s_2} - \vec{s_1}|. \tag{4}$$

As distances can be ambiguous in describing changes, the angle α between the two vectors is taken as a measure for shifts in the balance (b) of ecosystem processes which is calculated with:

$$b = 1 - \cos\alpha = 1 - \frac{\vec{s_1} \cdot \vec{s_2}}{|\vec{s_1}||\vec{s_2}|}. \tag{5}$$

If the direction of $\vec{s_1}$ and $\vec{s_2}$ is identical (and thus the relative contributions of all parameters are constant), $\cos\alpha = 1$, if they are orthogonal, $\cos\alpha = 0$ and if they are opposed, $\cos\alpha = -1$. Figure S4 (available at stacks.iop.org/ERL/6/034036/mmedia) illustrates this geometry for the two-dimensional case.

As the magnitude of state vector elements may differ by several orders, we normalize each variable to a mean value of 1. This preserves both the position of the zero point and the spread of the distribution, which contain essential information. In order to analyse relative ecosystem changes as well as their global importance, we use two different frames of reference:

For calculation of relative changes c, we calculate locally normalized state vectors $\vec{s_{l1}}$ and $\vec{s_{l2}}$, which have a mean value of 1 for the reference period at each point in space:

$$d_c = |\vec{s_{l_2}} - \vec{s_{l_1}}| \tag{6}$$

with

$$\vec{s_{l_1}} = \begin{pmatrix} 1 \\ 1 \\ \vdots \\ 1 \end{pmatrix}, \qquad \vec{s_{l_2}} = \begin{pmatrix} v_{1,l} \\ v_{2,l} \\ \vdots \\ v_{n,l} \end{pmatrix} \tag{7}$$

where

$$v_{i,l} = \frac{v_i}{\overline{v_{i,\mathrm{ref}}}}, \qquad \text{for } \overline{v_{i,\mathrm{ref}}} \neq 0 \tag{8}$$

and

$$\overline{v_{i,\mathrm{ref}}} = \frac{1}{m} \sum_{y=1}^{m} v_{i,y} \tag{9}$$

for reference years $y = 1, \ldots, m$.

Absolute changes d_g are calculated from globally normalized state vectors $\vec{s_{g1}}$ and $\vec{s_{g2}}$, which have a global mean value of 1 for the reference period, so that spatial patterns of variables are preserved and changes correspond to absolute changes in units of each variable's global mean value:

$$d_g = |\vec{s_{g_2}} - \vec{s_{g_1}}| \tag{10}$$

with

$$\vec{s_{g_1}} = \begin{pmatrix} v_{1,g,1} \\ v_{2,g,1} \\ \vdots \\ v_{n,g,1} \end{pmatrix}, \qquad \vec{s_{g_2}} = \begin{pmatrix} v_{1,g,2} \\ v_{2,g,2} \\ \vdots \\ v_{n,g,2} \end{pmatrix} \tag{11}$$

where each variable value is divided by the global, spatially averaged mean of the reference period:

$$v_{i,g,t} = \frac{v_{i,t}}{\overline{v_{i,\mathrm{refg}}}} \qquad \text{for } \overline{v_{i,\mathrm{refg}}} \neq 0 \tag{12}$$

with a global mean value

$$\overline{v_{i,\mathrm{refg}}} = \frac{1}{m \sum a_p} \sum_{p=1}^{z} \sum_{y=1}^{m} a_p \, v_{i,y,p} \tag{13}$$

for pixels $p = 1, \ldots, z$ with pixel area a_p.

Relative changes d_c and absolute changes d_g are scaled to a range between 0 and 1 to obtain metric components c and g using the following sigmoid function T:

$$c = T(d_c), \qquad g = T(d_g) \tag{14}$$

with

$$T(x) = A + \frac{1 - A}{1 + \mathrm{e}^{-6\ (x-0.5)}} \tag{15}$$

where $A = -\frac{1}{\mathrm{e}^3}$. This transformation assigns a value of 0 to 'no change' and a value $\geqslant$0.95 to changes with a magnitude larger than one mean value (local mean over the reference period for c, global mean for g). $S(x, \sigma_x)$ are sigmoid functions of the respective change-to-variability ratios of components x (c, g and b), with standard deviations σ_x within the reference period:

$$S(x, \sigma_x) = \frac{1}{1 + e^{-4(\frac{x}{\sigma_x} - 2)}}. \tag{16}$$

Changes within one standard deviation are hence assigned weights $S \leqslant 0.018$, changes of two standard deviations are weighted with 0.5 and changes beyond three standard deviations get weights $S \geqslant 0.982$.

2.2. Climate data

Climate projections from 22 GCMs, under forcing from the SRES A2, SRES A1B and SRES B1 emission scenarios (Nakicenovic *et al* 2000) are used as forcing data for LPJmL for the years 1901–2098. These models participated in the WCRP's CMIP phase 3 (https://esg.llnl.gov:8443/home/publicHomePage.do). Monthly fields of precipitation, surface air temperature and cloud cover are spatially interpolated to 1° resolution and bias-corrected (based on 1961–1990 bias) with an extended CRU TS2.1 climate dataset (Mitchell and Jones 2005, Oesterle *et al* 2003). Table S2 (available at stacks.iop.org/ERL/6/034036/mmedia) lists temperature and precipitation changes over land for all available climate projections. Projected climate patterns vary greatly between GCMs, especially for precipitation (figure S2 available at stacks.iop.org/ERL/6/034036/mmedia). Over large areas the models do not only disagree as to the magnitude of change, but even on its sign. Atmospheric carbon dioxide trajectories are taken from the BERN-CC carbon cycle model (www.ipcc-data.org/ancilliary/tar-bern.txt). Carbon dioxide concentrations in the year 2100 reach 836 ppm (A2), 703 ppm (A1B) and 540 ppm (B1), respectively.

2.3. The LPJmL model

For this study we employ the LPJmL DGVM as described by Sitch *et al* (2003) and Gerten *et al* (2004) with modifications made to general model features when implementing the LPJmL version with agriculture (Bondeau *et al* 2007). Here we employed LPJmL to simulate ecosystem state development under the given climate trajectories starting from a steady state. The model simulates key physiological and ecological processes based on a representation of nine PFTs. It is able to reproduce key features of the global carbon cycle (Jung *et al* 2008, Luyssaert *et al* 2010) and water cycle (Wagner *et al* 2003, Gerten *et al* 2004), vegetation patterns (Cramer *et al* 2001, Hickler *et al* 2006), plant phenology (Lucht *et al* 2002) and fire patterns (Thonicke *et al* 2001) and it has a CO_2-sensitivity within the range of FACE experiments (Gerten *et al* 2005, Hickler *et al* 2008). We did not analyse changes on agricultural areas (which may be affected differently by climate change), but since almost all grid cells contain at least a small fraction of natural vegetation, the resulting Γ values—which are independent of the actual area—are valid at every location. For a more detailed description of LPJmL see the supplementary information (SI available at stacks.iop.org/ERL/6/034036/mmedia).

2.4. Simulation design and presentation of results

LPJmL was spun up over 1000 years repeating years 1901–1930 of an extended CRU TS2.1 climate dataset (Oesterle *et al* 2003), followed by transient runs for all available climate trajectories for 1901–2098. Simulated ecosystem state is averaged for the reference period 1961–90 and for 2069–98, and its natural variability is calculated for 1961–90. Grid cells with vegetation cover below 10% in both time periods are excluded from the analysis, these regions represent deserts. The generic ecosystem stability index Γ (equation (1)) is computed for the variable subsets 'carbon fluxes', 'stored carbon', 'water' and 'all' (specified in table 1) between the future and reference period. Results for the subset 'all' over the 58 available climate trajectories are grouped into Koeppen's four main climate zones: tropical (Af, Aw, Am), dry (BS, BW), temperate (C, Cf, Cw, Cs) and cold (D, Df, Dw, ET, EF) based on classification of an average 1961–90 climate. Climate response functions $\Gamma = f(dT, d\mathrm{Prec})$ are fitted as second order polynomials to these data (within the range covered by the projected precipitation and temperature changes, excluding the upper and lower 1%). Risk of ecosystem changes is estimated based on the proportion of ecosystem projections showing considerable ($\Gamma > 0.3$) or small ($\Gamma < 0.1$) change and the uncertainty in climate projections.

3. Results

3.1. Dimensions of ecosystem change

Figure 1 shows the dimensions of change in detail for carbon and water fluxes as a mean of all climate scenarios. Local, relative changes (c) are found to be strongest in drought-stressed regions, where biomass and net primary production

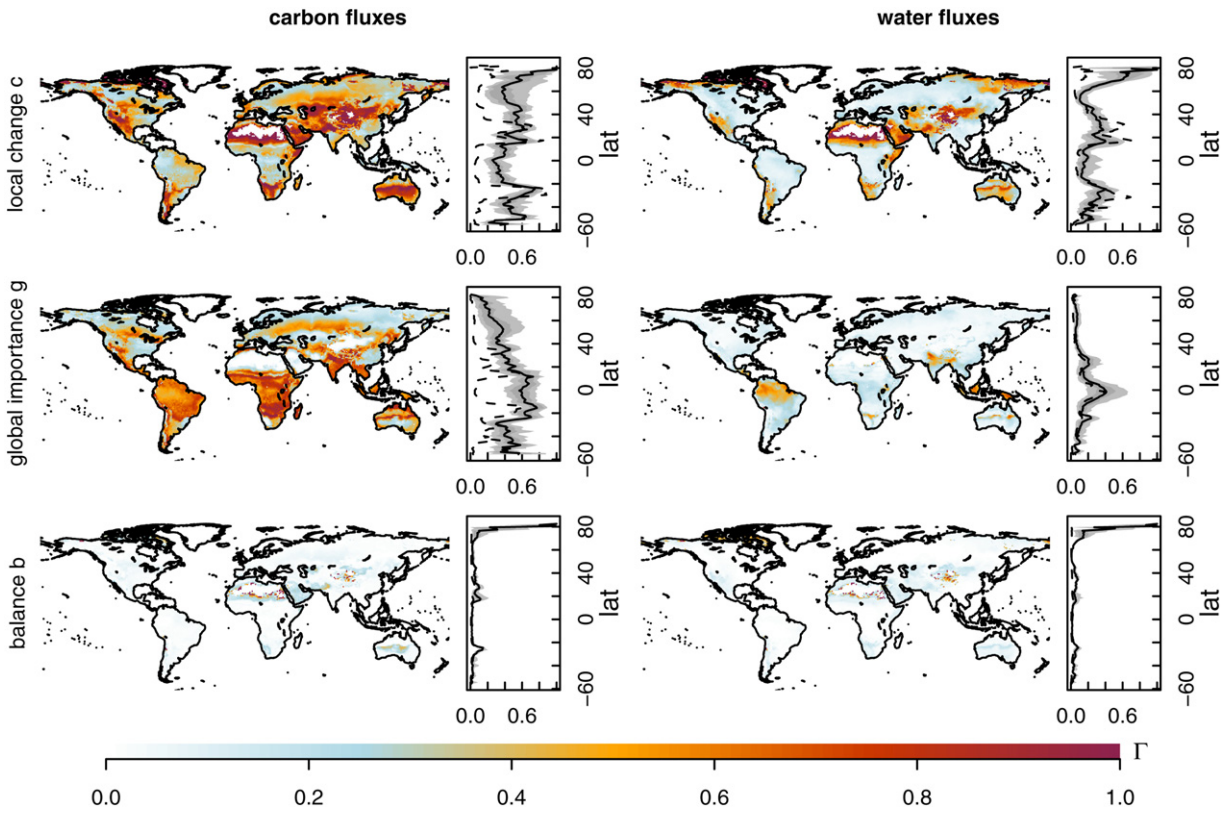

Figure 1. Components of the generic stability index Γ for carbon (left) and water fluxes (right). Median across climate projections and latitudinal averages, with model median (black line), 90% interval (grey) and interannual standard deviation 1961–90 (dashed line). Local change *c* (top), global importance *g* (middle) and balance *b* (bottom).

(NPP) are currently low but could increase in the future due to the effects of CO_2 fertilization. Projected absolute changes (g) in carbon fluxes at grid cell scale often reach a magnitude close to the current global mean value, while in case of water fluxes absolute magnitudes are generally rather low compared to the global mean. Changes in carbon fluxes exceed interannual variability substantially, while changes in water fluxes in many regions are close to the standard deviation of the reference period. Uncertainty among climate models is far greater for projections of water fluxes than for carbon fluxes.

Spatial patterns of projected changes in ecosystem properties vary greatly (figure 2), depending on the variable subsets considered (table 1). Vegetation structure changes little on average across different climate projections in the tropics, but quite strongly in the boreal–temperate ecotone: as boreal PFTs become increasingly heat-stressed, their mortality rates increase, and eventually they cannot be replaced fast enough by temperate PFTs. Carbon fluxes change considerably over large areas, which is caused by drought-related increases in fire frequency, by temperature-driven increases in soil respiration and/or by CO_2 fertilization effects on NPP. Stored carbon is most sensitive in the high latitudes, where soil carbon stocks decrease, and in the tropics and subtropics where biomass stocks increase. Across climate projections, water fluxes change little on average, although variability between projections is very high in the tropics, including the possibility of severe changes in some regions in single climate change projections.

Table 2. Projected ecosystem change Γ, 2069–2098 to 1961–1990, model average (model range) for each continent and emission pathway.

	A2	A1B	B1
Africa	0.28 (0.23–0.36)	0.25 (0.2–0.32)	0.17 (0.14–0.22)
Asia	0.25 (0.2–0.31)	0.22 (0.17–0.29)	0.15 (0.11–0.2)
Australia	0.26 (0.15–0.38)	0.24 (0.15–0.37)	0.16 (0.12–0.22)
Europe	0.18 (0.14–0.26)	0.15 (0.12–0.22)	0.1 (0.07–0.13)
North-America	0.24 (0.17–0.37)	0.21 (0.16–0.32)	0.15 (0.11–0.25)
South-America	0.26 (0.19–0.33)	0.23 (0.16–0.3)	0.15 (0.11–0.25)
Global	0.25 (0.21–0.31)	0.22 (0.17–0.28)	0.15 (0.12–0.2)

While the high-emission A2 and A1B scenarios suggest similarly strong impacts on ecosystems, the lower-emission B1 scenario shows considerably smaller changes on all continents (table 2). Ecosystems in Europe change the least on average and variation among climate models is small; larger changes are projected for all other continents for all emission pathways. Figures S1 and S3 (available at stacks.iop.org/ERL/6/034036/mmedia) show the spatial distribution and contributions of change dimensions in more detail.

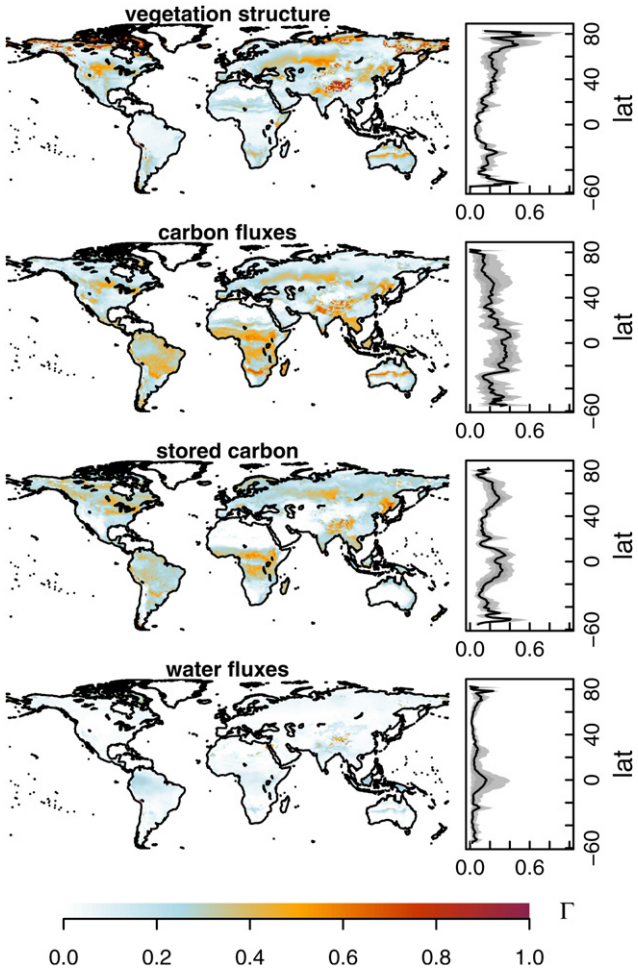

Figure 2. Spatial patterns (left, mean of 58 climate projections) and latitudinal averages (right, model median (black line) and 90% interval (grey)) of ecosystem changes Γ for the variable subsets 'vegetation structure', 'carbon fluxes', 'stored carbon' and 'water fluxes' (specified in table 1). A value of $\Gamma \geqslant 0.3$ denotes severe ecosystem change.

3.2. Climate response functions of ecosystems

Climate sensitivity of ecosystems—derived by fitting response functions to all locations in a given Koeppen climate group across 58 climate projections—varies strongly across climate zones (figure 3): cold climate ecosystems show a high sensitivity to temperature changes but a low sensitivity to precipitation changes, whereas dryland ecosystems show opposite sensitivities. In temperate and tropical ecosystems the sensitivity to changes in precipitation depends on temperature change: strong warming increases the sensitivity to declining precipitation.

Small ecosystem changes ($\Gamma < 0.1$) can only be expected in temperate or tropical regions at local temperature increases below 2 K with constant or slightly declining precipitation. Cold climate ecosystems—which are usually temperature limited—respond already at such low temperature changes. Local temperature changes around 4 K, which are projected by most climate models for the boreal zone for the end of the 21st century even under the moderate B1 emission scenario, will according to our simulations lead to moderate

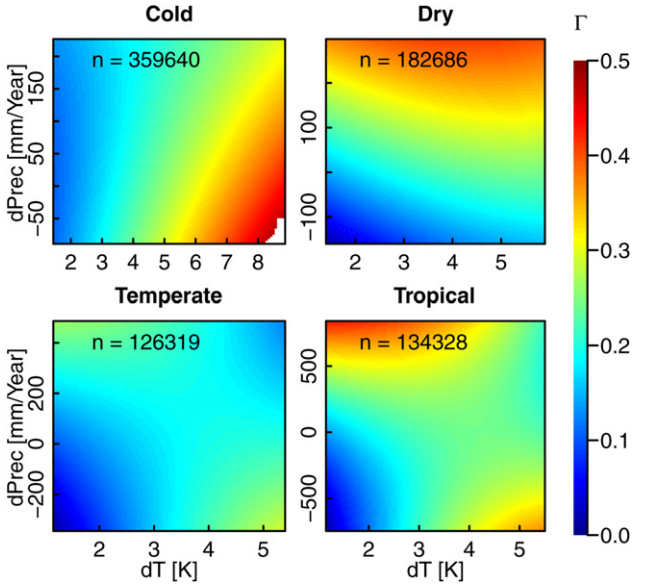

Figure 3. Climate response functions of ecosystems in different climate zones. Plotted local precipitation change (y-axis) against local temperature changes (x-axis).

but still substantial ecosystem changes ($\Gamma \sim 0.25$). Note, since local temperature changes deviate from the global mean temperature change, local temperature change will be larger in most regions.

3.3. Risk of overall ecosystem change

Considerable responses of ecosystems to changing climate (Γ for 'all', figure 4(a)) are most likely in the temperate–boreal ecotone, where boreal tree populations might become increasingly heat-stressed and replaced by better adapted temperate species/variations, in tundra regions where the tree line advances northward due to increased temperatures, and in some dry areas, where an elevated CO_2 concentration enhances plants' water use efficiency. Severe changes are unlikely (<5% of 58 climate projections) only in a core zone of the boreal biome, in moist tropical forests of Africa and South-East Asia and in deserts.

Limited ecosystem changes (figure 4(b)) are projected consistently across climate projections for arid and semi-arid regions and some parts of the US, Europe and China. Some projections show limited changes also for the humid tropics of South America, African savannah regions or a core zone of the boreal region. The uncertainty in ecosystem responses across variations between climate models and emission pathways (Figure 4(c)) is very high in many regions (e.g. Latin America, Sahel, southern Africa, Indian subcontinent, Australia), ranging from 'no change' up to complete restructuring of ecosystems (cf uncertainty in precipitation projections, figure S2 available at stacks.iop.org/ERL/6/034036/mmedia).

4. Discussion

We find from an analysis encompassing all available WCRP CMIP3 climate model projections that almost any region of

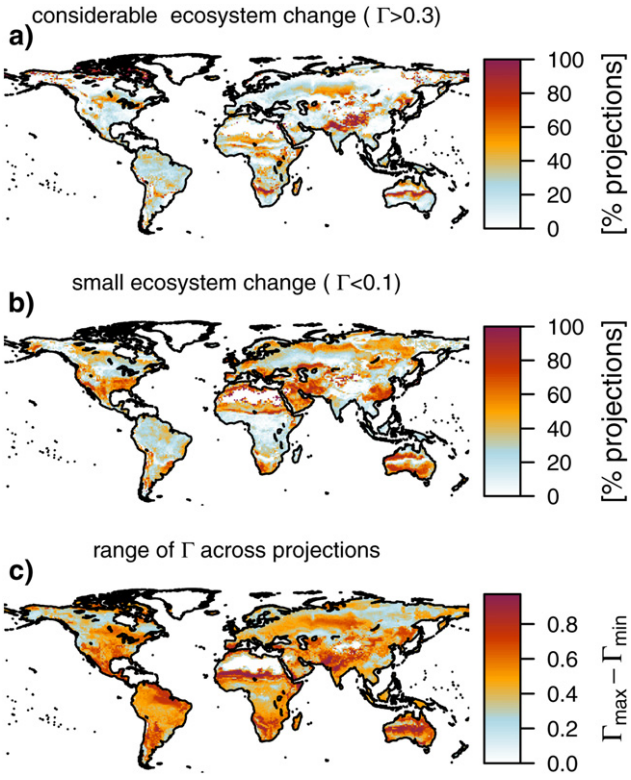

Figure 4. Percentage of climate projections showing (a) severe ecosystem change ($\Gamma > 0.3$), (b) small ecosystem change ($\Gamma < 0.1$) and (c) range of Γ across climate projections.

the world could be affected by severe ecosystem changes, particularly the boreal and temperate zones outside Europe and water-limited regions. Boreal forests change at their leading edge due to alleviated temperature limits and at their trailing edge due to increasing heat and drought stress. Such heat- and drought-related forest die-back (which might be amplified by insect outbreaks) has already been observed over considerable areas in North America (Berg *et al* 2006, Allen *et al* 2010). Dryland ecosystems are projected to experience increased vegetation productivity. This is in line with the known beneficial effect of elevated atmospheric CO_2 concentration on the water use efficiency of plants (Ainsworth and Long 2005), which will—together with warming—lead to increasing NPP and vegetation carbon stocks in many regions. In this study a major factor is not included: NPP could be constrained by nitrogen supply and other nutrients (Norby *et al* 2010), so that the increased NPP due to enhanced CO_2 availability as implied in our results should be interpreted as a maximum effect. LPJmL uses an optimized leaf allocation scheme to maximize the carbon uptake by regulating carbon fixation and respiration, which has been shown by Hickler *et al* (2008) to model realistically the CO_2 effect on NPP if other limitations are absent.

However, there is no robust knowledge about how individual ecosystem features and processes will respond to such a massive increase in available energy. For example, competitive conditions among species may change drastically, favouring some species and disadvantaging others. We are aware that DGVMs do not explicitly quantify species-level and small-scale processes pending generalized, globally applicable knowledge about such processes. Nonetheless, our ecosystem change metric Γ implicitly estimates the risk of unpredictable ecosystem breakdowns based on robustly modelled physiological processes—given the assumption that severe changes in either component of Γ or concurrent changes in several components are indicators of change in further ecosystem processes that are not explicitly quantified. The impact of land use on Γ should be further investigated; here we restrict our investigation on natural vegetation only to expose the impact of climate change on it.

Considerable changes ($\Gamma > 0.25$) of cold climate and tropical ecosystems could become likely around 3 K local temperature increase; temperate ecosystems will change considerably at local temperature increases above 4 K. Given that mean global warming is now rather unlikely to be prevented from exceeding 2 K (Rogelj *et al* 2010), substantial changes in the world's ecosystems can be expected in the course of this century. In view of the uncertainties involved at all stages—from uncertainty in forcing, magnitude and pattern of climate change projections to vegetation model realism and underlying ecophysiological process understanding—we merely argue that large values of our metric Γ indicate an increased risk of potential (but then serious) ecosystem disruption. We interpret our findings such that on the basis of best current knowledge from dynamic global biogeochemical and climate change models one cannot confidently preclude that in these cases such disruptions may occur. Whether such a risk of landscape change is acceptable to affected societies is open for discussion, but uncertainty in the analysis should not distract from the potential for large-scale change to occur. In any case, biospheric transformations, as indicated here by shifts in macroscopic ecosystem indicators, are likely to induce shifts also in human societies living in the respective landscapes. As humankind aims to scientifically understand the nature of the planetary boundaries within which societies should operate (Rockström *et al* 2009), awareness of the transformations caused by climate change in the living environment are an important factor. Mitigation pathways currently achieved and prospectively considered in political negotiations do not limit climate change to a magnitude where such ecosystem change is precluded.

Acknowledgments

This study was funded by the WGL's initiative 'Pakt für Forschung', the BMBF's GLUES project, and the European Community's ENSEMBLES, ERMITAGE and WATCH Integrated Projects. We acknowledge the climate modelling groups, the Program for Climate Model Diagnosis and Intercomparison (PCMDI) and the WCRP's Working Group on Coupled Modelling (WGCM) for making available the WCRP CMIP3 multi-model dataset; support of this dataset is provided by the Office of Science, US Department of Energy. We thank the PIK LPJ group for fruitful discussions.

References

Ainsworth E A and Long S P 2005 What have we learned from 15 years of free-air CO_2 enrichment (FACE)? A meta-analytic

review of the responses of photosynthesis, canopy properties and plant production to rising CO_2 *New Phytol.* **165** 351–72
Allen C D *et al* 2010 A global overview of drought and heat-induced tree mortality reveals emerging climate change risks for forests *Forest Ecol. Manag.* **259** 660–84
Berg E E, Henry J D, Fastie C L, Volder A D D and Matsuoka S M 2006 Spruce beetle outbreaks on the Kenai Peninsula, Alaska, and Kluane National Park and Reserve, Yukon Territory: Relationship to summer temperatures and regional differences in disturbance regimes *Forest Ecol. Manag.* **227** 219–32
Betts R A, Cox P M, Collins M, Harris P P, Huntingford C and Jones C D 2004 The role of ecosystem-atmosphere interactions in simulated amazonian precipitation decrease and forest dieback under global climate warming *Theor. Appl. Climatol.* **78** 157–75
Bondeau A *et al* 2007 Modelling the role of agriculture for the 20th century global terrestrial carbon balance *Glob. Change Biol.* **13** 679–706
Chapin F S *et al* 2005 Role of land-surface changes in Arctic summer warming *Science* **310** 657–60
Cramer W *et al* 2001 Global response of terrestrial ecosystem structure and function to CO_2 and climate change: results from six Dynamic Global Vegetation Models *Glob. Change Biol.* **7** 357–73
Ernest S K M and Brown J H 2011 Homeostasis and compensation: the role of species and resources in ecosystem stability *Ecology* **82** 2118–32
Foley J A, Prentice I C, Ramankutty N, Levis S, Pollard D, Sitch S and Haxeltine A 1996 An integrated biosphere model of land surface processes, terrestrial carbon balance, and vegetation dynamics *Glob. Biogeochem. Cycles* **10** 603–28
Friedlingstein P 2006 Climate-carbon cycle feedback analysis: results from the (CMIP)-M-4 model intercomparison *J. Clim.* **19** 3337–53
Gerten D, Hoff H, Bondeau A, Lucht W, Smith P and Zaehle S 2005 Contemporary 'green' water flows: simulations with a dynamic global vegetation and water balance model *Phys. Chem. Earth* A/B/C **30** 334–8
Gerten D, Schaphoff S, Haberlandt U, Lucht W and Sitch S 2004 Terrestrial vegetation and water balance—hydrological evaluation of a dynamic global vegetation model *J. Hydrol.* **286** 249–70
Gerten D, Schaphoff S and Lucht W 2007 Potential future changes in water limitations of the terrestrial biosphere *Clim. Change* **80** 277–99
Hickler T, Prentice I C, Smith B, Sykes M T and Zaehle S 2006 Implementing plant hydraulic architecture within the LPJ Dynamic Global Vegetation Model *Glob. Ecol. Biogeography* **15** 567–77
Hickler T, Smith B, Prentice I C, Mjöfors K, Miller P, Arneth A and Sykes M T 2008 CO_2 fertilization in temperate FACE experiments not representative of boreal and tropical forests *Glob. Change Biol.* **14** 1531–42
Jung M, Verstraete M, Gobron N, Reichstein M, Papale D, Bondeau A, Robustelli M and Pinty B 2008 Diagnostic assessment of European gross primary production *Glob. Change Biol.* **14** 2349–64
Krinner G, Viovy N, de Noblet-Ducoudré N, Ogée J, Polcher J, Friedlingstein P, Ciais P, Sitch S and Prentice I C 2005 A dynamic global vegetation model for studies of the coupled atmosphere-biosphere system *Glob. Biogeochem. Cycles* **19** GB1015
Lenton T M, Held H, Kriegler E, Hall J W, Lucht W, Rahmstorf S and Schellnhuber H J 2008 Tipping elements in the earth's climate system *Proc. Natl Acad. Sci.* **105** 1786–93
Lucht W, Prentice I C, Myneni R B, Sitch S, Friedlingstein P, Cramer W, Bousquet P, Buermann W and Smith B 2002 Climatic control of the high-latitude vegetation greening trend and pinatubo effect *Science* **296** 1687–9
Luyssaert S *et al* 2010 The European carbon balance. part 3: forests *Glob. Change Biol.* **16** 1429–50
McGuire A D *et al* 2001 Carbon balance of the terrestrial biosphere in the twentieth century: Analyses of CO_2, climate and land use effects with four process-based ecosystem models *Glob. Biogeochem. Cycles* **15** 183–206
Mitchell T D and Jones P D 2005 An improved method of constructing a database of monthly climate observations and associated high-resolution grids *Int. J. Climatol.* **25** 693–712
Nakicenovic N *et al* 2000 *Special Report on Emissions Scenarios: a Special Report of Working Group III of the Intergovernmental Panel on Climate Change* (Cambridge: Cambridge University Press) pp 590–662
Norby R J, Warren J M, Iversen C M, Medlyn B E and McMurtrie R E 2010 CO_2 enhancement of forest productivity constrained by limited nitrogen availability *Proc. Natl Acad. Sci.* **107** 19368–73
Oesterle H, Gerstengarbe F and Werner P C 2003 Homogenisierung und aktualisierung des klimadatensatzes der Climate Research Unit der University of East Anglia, Norwich *Terra Nostra* **2003/6** 326–9
Parmesan C 2006 Ecological and evolutionary responses to recent climate change *Annu. Rev. Ecol. Evol. Syst.* **37** 637–69
Randall D A *et al* 2007 Climate models and their evaluation *Climate Change 2007: The Physical Science Basis. Contribution of Working Group I to the Fourth Assessment Report of the Intergovernmental Panel on Climate Change* ed S Solomon *et al* (Cambridge: Cambridge University Press) pp 589–662
Rockström J *et al* 2009 A safe operating space for humanity *Nature* **461** 472–5
Rogelj J, Nabel J, Chen C, Hare W, Markmann K, Meinshausen M, Schaeffer M, Macey K and Hohne N 2010 Copenhagen accord pledges are paltry *Nature* **464** 1126–8
Scheffer M, Carpenter S, Foley J A, Folke C and Walker B 2001 Catastrophic shifts in ecosystems *Nature* **413** 591–6
Scholze M, Knorr W, Arnell N W and Prentice I C 2006 A climate-change risk analysis for world ecosystems *Proc. Natl Acad. Sci.* **103** 13116–20
Sitch S *et al* 2003 Evaluation of ecosystem dynamics, plant geography and terrestrial carbon cycling in the LPJ dynamic global vegetation model *Glob. Change Biol.* **9** 161–85
Sykes M T, Prentice I C and Laarif F 1999 Quantifying the impact of global climate change on potential natural vegetation *Clim. Change* **41** 37–52
Thonicke K, Venevsky S, Sitch S and Cramer W 2001 The role of fire disturbance for global vegetation dynamics: coupling fire into a Dynamic Global Vegetation Model *Glob. Ecol. Biogeography* **10** 661–77
Wagner W, Scipal K, Pathe C, Gerten D, Lucht W and Rudolf B 2003 Evaluation of the agreement between the first global remotely sensed soil moisture data with model and precipitation data *J. Geophys. Res.* **108** 4611
Williams J W, Jackson S T and Kutzbach J E 2007 Projected distributions of novel and disappearing climates by 2100 AD *Proc. Natl Acad. Sci.* **104** 5738–42
Woodward F I, Smith T M and Emanuel W R 1995 A global land primary productivity and phytogeography model *Glob. Biogeochem. Cycles* **9** 471–90